HOSTED BY

ELSEVIER

Available online at www.sciencedirect.com

ScienceDirect

Journal of Sport and Health Science 11 (2022) 495–508

Original article

Exercise promotes angiogenesis by enhancing endothelial cell fatty acid utilization via liver-derived extracellular vesicle miR-122-5p

Jing Lou [a,b,†], Jie Wu [b,c,†], Mengya Feng [a,b], Xue Dang [b], Guiling Wu [b], Hongyan Yang [b], Yan Wang [a], Jia Li [b], Yong Zhao [d], Changhong Shi [d], Jiankang Liu [a], Lin Zhao [a,*], Xing Zhang [b,*], Feng Gao [b]

[a] *Center for Mitochondrial Biology and Medicine, The Key Laboratory of Biomedical Information Engineering of Ministry of Education, School of Life Science and Technology, Xi'an Jiaotong University, Xi'an 710049, China*

[b] *School of Aerospace Medicine, Fourth Military Medical University, Xi'an 710032, China*

[c] *Medical School of Chinese PLA, Beijing 100853, China*

[d] *Laboratory Animal Center, Fourth Military Medical University, Xi'an 710032, China*

Received 1 May 2021; revised 17 June 2021; accepted 3 August 2021

Available online 1 October 2021

Abstract

Background: Angiogenesis constitutes a major mechanism responsible for exercise-induced beneficial effects. Our previous study identified a cluster of differentially expressed extracellular vesicle microRNAs (miRNAs) after exercise and found that some of them act as exerkines. However, whether these extracellular vesicle miRNAs mediate the exercise-induced angiogenesis remains unknown.

Methods: A 9-day treadmill training was used as an exercise model in C57BL/6 mice. Liver-specific adeno-associated virus 8 was used to knock down microRNA-122-5p (miR-122-5p). Human umbilical vein endothelial cells were used *in vitro*.

Results: Among these differentially expressed extracellular vesicle miRNAs, miR-122-5p was identified as a potent pro-angiogenic factor that activated vascular endothelial growth factor signaling and promoted angiogenesis both *in vivo* and *in vitro*. Exercise increased circulating levels of miR-122-5p, which was produced mainly by the liver and shuttled by extracellular vesicles in mice. Inhibition of circulating miR-122-5p or liver-specific knockdown of miR-122-5p significantly abolished the exercise-induced pro-angiogenic effect in skeletal muscles, and exercise-improved muscle performance in mice. Mechanistically, miR-122-5p promoted angiogenesis through shifting substrate preference to fatty acids in endothelial cells, and miR-122-5p upregulated endothelial cell fatty-acid utilization by targeting 1-acyl-sn-glycerol-3-phosphate acyltransferase (AGPAT1). In addition, miR-122-5p increased capillary density in perilesional skin tissues and accelerated wound healing in mice.

Conclusion: These findings demonstrated that exercise promotes angiogenesis through upregulation of liver-derived extracellular vesicle miR-122-5p, which enhances fatty acid utilization by targeting AGPAT1 in endothelial cells, highlighting the therapeutic potential of miR-122-5p in tissue repair.

Keywords: Angiogenesis; Endothelial cells; Exerkine; Extracellular vesicle; Metabolic shift

1. Introduction

It is well established that physical inactivity initiates maladaptations that increase the risks of various diseases.[1] In contrast, regular physical activity not only reduces risk of diseases but also activates the endogenous "medkit" to cure diseases, including myocardial infarction, peripheral arterial disease, osteoporosis, and others.[2,3] Evidence has shown that promotion of angiogenesis, which increases the blood flow and energy supply to tissues, constitutes a major mechanism responsible for exercise-induced beneficial effects in both physiological and pathological conditions.[4,5] It has been shown that even a short term of exercise leads to a ~5-fold increase in blood flow and a 20% increase in capillary density in skeletal muscles.[6,7]

The process of angiogenesis is regulated by a balance between pro- and anti-angiogenesis factors.[5] In response to pro-angiogenic stimuli such as exercise, vascular endothelial cells (ECs) are activated to migrate to distant sites and

Peer review under responsibility of Shanghai University of Sport.

* Corresponding authors.
E-mail addresses: zhaolin2015@mail.xjtu.edu.cn (L. Zhao), zhangxing@fmmu.edu.cn (X. Zhang).
† These authors contributed equally to this study.

https://doi.org/10.1016/j.jshs.2021.09.009

Cite this article: Lou J, Wu J, Feng M, et al. Exercise promotes angiogenesis by enhancing endothelial cell fatty acid utilization via liver-derived extracellular vesicle miR-122-5p. *J Sport Health Sci* 2022;11:495–508.

proliferate to form new primary capillaries.[8,9] Impaired EC angiogenic responses have been linked to impaired tissue repair[10] and exacerbation of a wide range of diseases.[8,11] Although multiple cytokines, including fibroblast growth factor, placenta growth factor, platelet-derived growth factor, and transforming growth factor β, are involved in angiogenesis, vascular endothelial growth factor (VEGF) appears to be the central factor in initiating angiogenesis.[5] Both long-term and short-term exercise upregulates VEGF signaling and capillarity in skeletal muscles.[5] However, how exercise orchestrates the complex process of physiological angiogenesis remains unknown. Recent studies have identified exerkines, which are secreted from multiple tissues in response to exercise, as major players in orchestrating cell-to-cell crosstalk and mediating the exercise-induced beneficial effects.[12–14] Among exerkines, myokines, including interleukin 6, irisin, and apelin secreted from skeletal muscles, have been studied extensively.[15,16] Searching for exerkines provides a framework for understanding how exercise mediates many of its beneficial effects and provides a platform for pharmacotherapy development in various diseases.

Interest in this field has grown rapidly with the increased knowledge that numerous exerkines are shuttled by extracellular vesicles such as exosomes, the small (30−100 nm) endogenous membrane vesicles secreted by most cell types.[17,18] Recently, we found that although the total circulating extracellular vesicles did not change significantly postexercise, the isolated plasma extracellular vesicles from exercised animals afforded remarkable protection against myocardial ischemia/reperfusion injury.[19] MicroRNA (miRNA) sequencing identified 12 differentially expressed miRNAs in the circulating extracellular vesicles of exercised animals.[19] In this study, we found that 1 of these differentially expressed miRNAs, liver-derived extracellular vesicle miR-122-5p (previously named miR-122 or miR-122a), acts as a novel exerkine that contributes to exercise-promoted angiogenesis.

2. Methods

2.1. Animals and the exercise model

All animal studies were performed in accordance with national guidelines and were approved by the Fourth Military Medical University Animal Care and Use Committee, Xi'an, China. C57BL/6 mice (male) at the age of 8 weeks were purchased from the Experimental Animal Center of the Fourth Military Medical University, Xi'an, China. Mice were fed standard chow and housed under a 12 h light/12 h dark cycle. For the exercise model, mice were acclimatized to the treadmill for 3 consecutive days prior to the exercise training. For acclimatization, mice were subjected to exercise at 9 m/min for 20 min at 0° inclination, 10 m/min for 30 min at 0° inclination and 15 m/min for 40 min at 0° inclination on 3 different days. The animals were then trained at 18 m/min for 1 h at 0° inclination for 9 continuous days. For euthanasia, mice were anaesthetized with an intraperitoneal injection of sodium pentobarbital (100 mg/kg body weight, P-010; Merck, Darmstadt, Hesse, Germany) and then euthanized via exsanguination.

2.2. Matrigel plug assay

A Matrigel plug assay was used to examine angiogenesis *in vivo*, as described previously.[20] In brief, the mice were anesthetized with continuous 2% isoflurane (130302; Yipin Pharmaceutical, Shijiazhuang, China) in 1 L/min oxygen through a tight-fitting facemask (24002; Harvard Apparatus, Holliston, MA, USA) for 10 min, and the hind limbs were then sterilized. Agonist miRNA (agomiR)-negative control (NC) or agomiR-122-5p was synthesized by RiboBio (Guangzhou, China), and 100 nmoL/kg body weight agomiR were diluted with a 0.5 mL Matrigel matrix (35243; Corning, New York, NY, USA) and then implanted into the inguinal subcutaneous area of each mouse. The anesthesia was maintained in the mice for at least another 30 min to ensure that the Matrigel matrix was completely solidified. Mice were fed standard chow, and the Matrigel matrix (Coring) was taken out 1 week later.

2.3. AgomiRNA and antagomiRNA injection

AgomiR-NC, agomiR-122-5p, antagomiR-NC, and antagomiR-122-5p were synthesized by Ribobio. Either agomiR-NC or agomiR-122-5p was injected once (0.4 mg/kg body weight in 50 μL saline for each quadricep) into each quadricep at 4 points. Mice were euthanized with an intraperitoneal injection of sodium pentobarbital (100 mg/kg body weight; Merck) 3 days after quadriceps injection. Either antagomiR-NC or antagomiR-122-5p was injected (0.8 mg/kg body weight in 0.1 mL saline) into the tail vein every other day from the 1st day to the 9th day of treadmill training. The sequences of agomiRNAs and antagomiRNAs used is shown in Supplementary Table 1.

2.4. Adeno-associated virus injection

To determine whether liver-derived miR-122-5p contributes to exercise-induced angiogenesis, liver-specific adeno-associated virus 8 (AAV8) carrying the Mus musculus (mmu)-miR-122-5p reverse complementary sequence (5'-GAATTCCAAACACCATTGTCACACTCCATATACCAAACACCATTGTCACACTCCAACATCCAAACACCATTGTCACACTCCATCTTCACAAACACCATTGTCACACTCCATTTTTGGATCC-3') was packaged and synthesized by Hanbio Biotechnology (Shanghai, China). In brief, the anti-mmu-miR-122-5p sequence was cloned into a pHBAAV-U6-ZsGreen vector to form a pHBAAV-U6-ZsGreen-miR-122-5p vector. AAV8-anti-miR-122-5p viral particles were packaged in AAV-293 cells (Hanbio Biotechnology) using the pHBAAV-U6-ZsGreen-miR-122-5p vector, pAAV-RC vector, and pHelper vector. AAV8 viral particles carrying an empty vector were used as a negative control. The virus titer was 1.3×10^{12} v.g./mL. Each mouse was injected with 100 μL of AAV8 through the tail vein at 1 month before treadmill training. AAV8 injection efficiency was detected by quantitative polymerase chain reaction (qPCR).

2.5. Forelimb strength

A grip-strength meter (BIO-GS3; Bioseb, Pinellas Park, FL, USA) was used to measure the forelimb grip strength of the

mice. The mice were put on the grid, and their torsos were kept horizontal, allowing only the front paws to attach the grid. Then the mices' tails were gently pulled back, ensuring that their torsos were parallel to the grid so as to eliminate the interference of back strength. The forelimb grip strength of each mouse was measured 5 times discontinuously, and an average value was calculated.

2.6. Rotarod test

A rotarod system with 5 individual chambers (JLBehv-RRTG; Shanghai Jiliang Software Technology, Shanghai, China) was used to detect the motor coordination of mice. In brief, the mice were acclimated to the rotarod with 3 trials every day for a period of 3 days. The rotarod accelerated from 4 revolutions per minute (rpm) to 40 rpm in 5 min and maintained the maximum speed until the mice fell. Animals were scored for their latency to fall for each trial. The mice rested for a minimum of 10 min between trials to avoid fatigue.

2.7. Plasma extracellular vesicles isolation and analysis

The mice were euthanized 24 h after the last training session by an intraperitoneal injection of sodium pentobarbital (100 mg/kg body weight; Merck), and plasma and extracellular vesicles were collected as described previously.[19] Briefly, extracellular vesicles were separated by differential centrifugation. Blood samples were centrifuged at 1600 *g* for 20 min at 4°C to obtain plasma, followed by 10,000 *g* for 30 min to remove cells and platelets and at 100,000 *g* for 60 min twice to collect extracellular vesicles. The isolated extracellular vesicles were resuspended in phosphate-buffered saline (PBS, B548117; Sangon Biotech, Shanghai, China) for further study. Extracellular vesicles were visualized using transmission electron microscopy (H7500; Hitachi, Tokyo, Japan), as described previously.[19] Particle concentration was quantified using a NanoSight NS300 (Marvern Panalytical, Worcester, UK), as described previously.[19]

2.8. Wound healing

Mice were anesthetized by an intraperitoneal injection of sodium pentobarbital (50 mg/kg body weight; Merck), and their backs were shaved and cleaned. A sterile 6 mm skin biopsy punch (BP60; HealthLink, Oakland, CA, USA) was used to make 2 wounds in each mouse. Every 2 days, agomiR-NC or agomiR-122-5p (0.8 mg/kg body weight in 0.1 mL saline for each wound) was injected intradermally into the wound edges at 4 points in the mice. Wound closure was quantified by Image J software (1.50i; NIH, Bethesda, MD, USA) and calculated as the percentage of the original wound size. After the mice were euthanized by an intraperitoneal injection of sodium pentobarbital (100 mg/kg body weight; Merck), 5 mm of nonwounded perilesional skin from the margin of the wound site were collected for immunofluorescence and Western blot.

2.9. Cell lines

Human umbilical vein ECs were obtained from American Tissue Culture Collection. Cells were cultured in endothelial cell medium (ECM) containing 5% fetal bovine serum, 1% EC growth supplement, and 1% penicillin/streptomycin solution (1001; ScienCell, Carlsbad, CA, USA). Cells were grown under 5% CO_2 at 37°C.

2.10. Gene expression analysis

Total cellular RNA and small RNA were isolated using RNAiso (9753; Takara, Osaka, Japan) according to standard procedures. In serum samples, celworm (cel)-miR-39 (miRB0000010-3-1; Ribobio) was added to standardize the technical differences between samples before the chloroform step. RNA concentrations were verified on the NanoDrop Spectrophotometer (Thermo Fisher, Waltham, MA, USA). RNAs were reversed by Mir-X TM miRNA First-Stand Synthesis Kit (638313; Takara). qPCR was performed on a Bio-Rad Real-time PCR System (CFX96; BioRad, Hercules, CA, USA) by SYBR Premix Ex TaqTM II Kit (639676; Takara) according to the manufacturer's protocol. Relative mRNA expression levels were calculated using the $2^{-\Delta\Delta CT}$ method. The primers of mRNA or miRNA were synthesized by Sangon Biotech (Shanghai, China). The sequences used are shown in Supplementary Table 2.

2.11. Transfection

Transfection of miRNA mimics (50 nmol/L for cells, 200 nmol/L for aortic rings), miRNA inhibitors (200 nmol/L for cells), small interfering RNAs (siRNAs, 50 nmol/L for cells, 200 nmol/L for aortic rings), and their negative controls (50 nmol/L for cells, 200 nmol/L for aortic rings) was performed using Lipofectamine RNAiMAX (13778; Invitrogen, Carlsbad, CA, USA) and Opti-MEM (31985062; Gibco, Carlsbad, CA, USA) according to the manufacturers' instructions. After 8 h of transfection in cells or 24 h of transfection in aortic rings, the medium was changed to the ECM (ScienCell). The transfection efficient was detected by qPCR or Western blot at 60 h after transfection. The miRNA mimic sequences are shown in Supplementary Table 1, and small interference RNA (siRNA) sequences are shown in Supplementary Table 3.

2.12. Predicting the target genes of miR-122-5p

Target genes of miR-122-5p were predicted through the use of the miRDB (http://www.mirdb.org/), miRanda (http://www.mocrorna.org), and TargetScan (http://www.targetscan.org/) online databases. The target genes were identified by taking the intersection of the 3 databases. The database for annotation, visualization and integrated discovery (DAVID) gene function classification tool was then used to classify the function of the gene.

2.13. Cell viability assay

The endothelium cells were seeded in 96-well plates with a density of 0.4×10^4 cells/well after transfection. The cell counting kit-8 (CCK-8) (40203; Yeasen Biotech, Shanghai, China) was used to detect the cell viability. A 100 μL medium containing 10 μL CCK-8 was added into each well at 48 h after transfection. The optical density value was detected at 450 nm (FLUOstar

Omega; BMG Labtech, Ortenberg, Germany) after 2 h of incubation.

2.14. Wound-scratch assay

ECs were seeded in a 35 mm plastic disk with an Ibidi Culture-Insert chamber (81176; Ibidi, Gräfelfing, Germany), and the culture insert was moved until a confluent monolayer formed. The wound closure was monitored over the next 24 h, and images were captured at the same location using a Brightfield inverted microscope (CKX41; Olympus, Tokyo, Japan). The migration distance was calculated using Image J software (NIH).

2.15. Tube formation assay

A Matrigel basement membrane matrix was diluted 1:1 with ECM. The Matrigel matrix (Corning) was added to each well in 96-well plates (50 μL/well) by using precooled pipette tips, and the plate was placed in a 37˚C incubator for 30 min to solidify the Matrigel matrix. ECs were digested and resuspended with ECM, and 10,000 cells were then seeded per well. The formation of tubes was observed 4 h after seeding using a Brightfield inverted microscope (CKX41; Olympus). The number of tubes was quantified using Image J software with an angiogenesis analyzer tool.

2.16. Aortic ring assay

Aortic ring assay was assessed as described previously.[21] Briefly, the mice were euthanized by an intraperitoneal injection of sodium pentobarbital (100 mg/kg body weight; Merck), and their thoracic aortas were dissected. Surrounding fat and other connective tissues were cleaned away. The aortas were cut into ~0.5 mm wide rings and transfected overnight. The next day, each aortic ring was embedded in 50 μL of Matrigel matrix (Corning) in a 12-well plate, and vessel sprouting was stimulated by supplementing 5% fetal bovine serum and 100 μg/mL endothelial cell growth supplement (ECGS) in ECM. The medium was replaced once every other day. After 4 days of incubation, the photos of resulting sprouts were acquired using a Brightfield inverted microscope (CKX41; Olympus). The sprout length was calculated using Image J software (NIH).

2.17. Immuofluorescence

The fresh quadriceps or perilesional skin tissues were placed in a tissue base mold and covered with optimal cutting temperature compound (OCT 4583; Sakura Finetek, Tokyo, Japan). Transverse sections were sectioned at 8 μm thickness and stored in a −80˚C freezer before staining. The sections were fixed in precooled acetone for 10 min. The slides were then washed with PBS (Sangon) twice and permeabilized with 0.1% Triton (T8787; Sigma-Aldrich, St. Louis, MO, USA). The sections were washed with PBS, blocked with goat serum (16210064; Gibco) for 1 h and incubated overnight at 4˚C in primary antibodies diluted at 1:100. The slides were washed with PBS twice and incubated for 2 h at room temperature with secondary antibodies diluted at 1:500. The slides were then washed with PBS twice and incubated with 4′,6-diamidino-2-phenylindole (DAPI) to stain nucleus. The immunofluorescence images were visualized by confocal microscopy (LSM 800; Zeiss, Oberkochen, Germany). Antibodies against platelet/endothelial cell adhesion molecule-1 (PECAM-1/CD31, ab213175), Laminin (ab11575) were purchased from Abcam (Cambridge, MA, USA). Fatty acid translocase (FAT/CD36, 18836) and carnitine palmitoyl-transferase 1A (CPT1A, 15184) were purchased from Proteintech (Wuhan, China). 1-acyl-sn-glycerol-3-phosphate acyltransferase-beta-1 (AGPAT1, GTX55496) was purchased from GeneTex (Irvine, CA, USA).

2.18. Enzyme-linked immunosorbent assay (ELISA)

ELISA assays were performed to detect the concentration of VEGF in serum and culture medium of ECs using a commercial kit (Cusabio, Wuhan, China). The manufacturer's instructions were followed.

2.19. Measurement of oxygen consumption rate

An XF24 Extracellular Flux Analyzer (Seahorse Bioscience, North Billerica, MA, USA) was used to measure the oxygen consumption rate (OCR) of ECs. Cells were seeded in XF24 cell-culture plates (20,000 cells/well, 102042; Seahorse Bioscience). Cells were incubated in a Tyrode solution consisting of (in mmol/L) 137 NaCl, 5.4 KCl, 1.2 $MgCl_2$, 1.2 NaH_2PO_4, 1.8 $CaCl_2$, 5.6 glucose or 10 pyruvate, and 20 HEPES (pH 7.35, adjusted with NaOH). The Tyrode solution contains only 150 μmol/L palmitic acid (PA) (P9767; Sigma) without glucose during detection. Bioenergetics analyses were performed with the injection of oligomycin (1 μmol/L, 75351; Sigma), carbonilcyanide p-triflouromethoxyphenylhydrazone (FCCP, 1 μmol/L, C2920; Sigma), rotenone (1 μM, R8875; Sigma), and antimycin A (1 μmol/L, A8674; Sigma) sequentially. OCR was determined and adjusted by protein concentration. OCRs for basal respiration, ATP production, proton leak, and maximal respiration were calculated following the manufacturer's instructions.

2.20. Western blot

Protein content from all samples was quantified using a bicinchoninic acid protein assay kit (23225; Thermo Fisher). Western blot analysis was performed using standard procedures, was detected using an enhanced chemiluminescence western blotting detection kit (32106; Thermo Fisher), and was quantified by scanning densitometry. Antibodies against phosphorylated (p)-protein kinase B (Akt) (Ser473) (#4060), Akt (#4685), p-extracellular signal-regulated kinase (ERK) (Thr202/Tyr204) (#4370), ERK (#4695), VEGF receptor-2 (VEGFR2, #9698), p-VEGFR2 (Tyr1175) (#3770), β-actin (#4970), and glyceraldehyde-3-phosphate dehydrogenase (GAPDH, #5174) were purchased from Cell Signaling Technology (Danvers, MA, USA). CD36 (18836), CPT1A (15184), carnitine palmitoyl-transferase 1B (CPT1B; 22170), VEGF

(19003), apolipoprotein A1 (APOA1; 14427), and golgi matrix protein 130 (GM130; 11308) were purchased from Proteintech. AGPAT1 (GTX55496) was purchased from GeneTex. CD31 (ab213175), tumor susceptibility 101 (TSG101, ab125011), and CD81 (ab109201) were purchased from Abcam. GAPDH or β-actin was used as a loading control.

2.21. Fatty acids and glucose uptake

The cells were starved for 6 h in a serum-free medium before fatty acid or glucose uptake detection. Fatty acid uptake was detected using a fatty acid uptake kit from Sigma (MAK156), and the manufacturer's instructions were followed. For the glucose uptake assay, cells were incubated in 200 μM of 2-(N-(7-nitrobenz-2-oxa-1,3-diaxol-4-yl) amino)-2-deoxyglucose (2-NBDG, N13195; Invitrogen, Waltham, MA, USA) for 1 h and washed with PBS 3 times. The fluorescence value was recorded at the excitation/emission of 488 nm/520 nm.

2.22. Luciferase reporter assay

As described previously,[19] a luciferase reporter assay was used to validate the mRNA target of miR-122-5p.

2.23. Statistical evaluation

All values are presented as mean ± SEM of independent experiments. The results were compared with one-way analysis of variance (ANOVA) or two-way ANOVA, with all ANOVA tests followed by an unpaired, 2-tailed *t* test, as appropriate. The Kolmogorov-Smirnov normality test was used to analyze the normal distribution of the data. A Bonferroni correction for multiple comparisons was used, $p < 0.05$ was considered to indicate a significant difference.

3. Results

3.1. miR-122-5p stood out as a potent miRNA in the promotion of angiogenesis in vitro and in vivo

We previously identified 12 differentially expressed miRNAs in circulating extracellular vesicles postexercise by using miRNA sequencing combined with qPCR.[19] After transfection of ECs with these miRNA mimics, cell viability was detected as a screening test to determine which miRNAs are potential regulators of angiogenesis. Among these miRNAs, the miR-122-5p mimic increased cell viability (Fig. 1A and 1B) and activated VEGF signaling as evidenced by the increased contents of VEGF, p-VEGFR2/VEGFR2, p-ERK/ERK, p-Akt, and Akt in cultured ECs (Fig. 1C), suggesting miR-122-5p as a potential pro-angiogenic factor. In addition, the miR-122-5p mimic increased VEGF secretion in cultured ECs (Supplementary Fig. 1). The pro-angiogenesis effect of miR-122-5p was further confirmed by the scratch, tube formation, and aortic ring sprouting assays. As shown in Fig. 1D−1F, the miR-122-5p mimic promoted cell migration and tube-like network formation in cultured ECs and increased aortic ring sprouting in cultured aortic rings. Furthermore, the miR-122-5p mimic displayed a dose-dependent effect on pro-angiogenesis in ECs (Supplementary Fig. 2). These results suggest that miR-122-5p is a potential pro-angiogenesis factor.

To test whether miR-122-5p promotes angiogenesis *in vivo*, 3 models were employed. First, mouse quadriceps muscle was injected with agomiR-NC or agomiR-122-5p to test whether miR-122-5p upregulation promotes angiogenesis in skeletal muscles (Fig. 1G). Three days after injection, agomiR-122-5p showed no significant effects on quadriceps muscle weight (Fig. 1H), but it increased capillary density in quadriceps muscles compared with quadriceps muscles injected with agomiR-NC (Fig. 1I). Meanwhile, agomiR-122-5p increased the contents of CD31, VEGF, and p-VEGFR2 in quadriceps muscles (Fig. 1J). In the second set of experiments, Matrigel was injected together with agomiR-NC or agomiR-122-5p subcutaneously in the inguinal space of mice. Seven days after injection, newly formed blood vessels were observed in the Matrigel plug, and these were increased by agomiR-122-5p (Fig. 1K and Fig. S3). Furthermore, an *in vivo* wound-healing model was used to test whether agomiR-122-5p promotes wound healing in mice. As shown in Fig. 1L and 1M, agomiR-122-5p treatment accelerated wound closure and increased capillary density in perilesional skin tissues. These results further indicate that miR-122-5p is a pro-angiogenic factor.

3.2. Exercise promoted angiogenesis through upregulation of circulating miR-122-5p

Exercise upregulated the circulating miR-122-5p levels after 9 days of training (Fig. 2A). We used antagomiR-122-5p to test whether miR-122-5p mediates the exercise-induced angiogenesis in skeletal muscles (Fig. 2B). AntagomiR-122-5p blocked the upregulation of circulating miR-122-5p induced by exercise (Fig. 2C). Neither exercise nor antagomiR-122-5p showed any significant effects on the body weight or muscle weight of the mice (Fig. 2D and 2E). Exercise increased the muscle performance as evidenced by the increased forelimb grip strength and motor coordination (Fig. 2F and 2G). However, these effects were abolished by antagomiR-122-5p (Fig. 2F and 2G). In addition, exercise increased expression levels of CD31 and VEGF in skeletal muscles and the capillary density, while these effects were abolished by antagomiR-122-5p (Fig. 2H and 2I). AntagomiR-122-5p also abolished the effects of exercise on upregulation of circulating VEGF (Supplementary Fig. 1). These results suggest that exercise-promoted angiogenesis in skeletal muscles is mediated by upregulation of miR-122-5p.

3.3. Exercise-upregulated miR-122-5p was shuttled by extracellular vesicles and derived from the liver

Extracellular vesicles were purified from the plasma of mice to test whether miR-122-5p is shuttled by extracellular vesicles. Electron microscopy analysis revealed typical rounded particles in isolated fractions (Fig. 3A). Nanoparticle tracking analysis displayed no significant differences in size distribution or plasma concentration, and Western blot analysis showed no significant differences in extracellular vesicle positive markers (TSG101 and CD81) and negative markers (APOA1 and GM130) between extracellular vesicles isolated

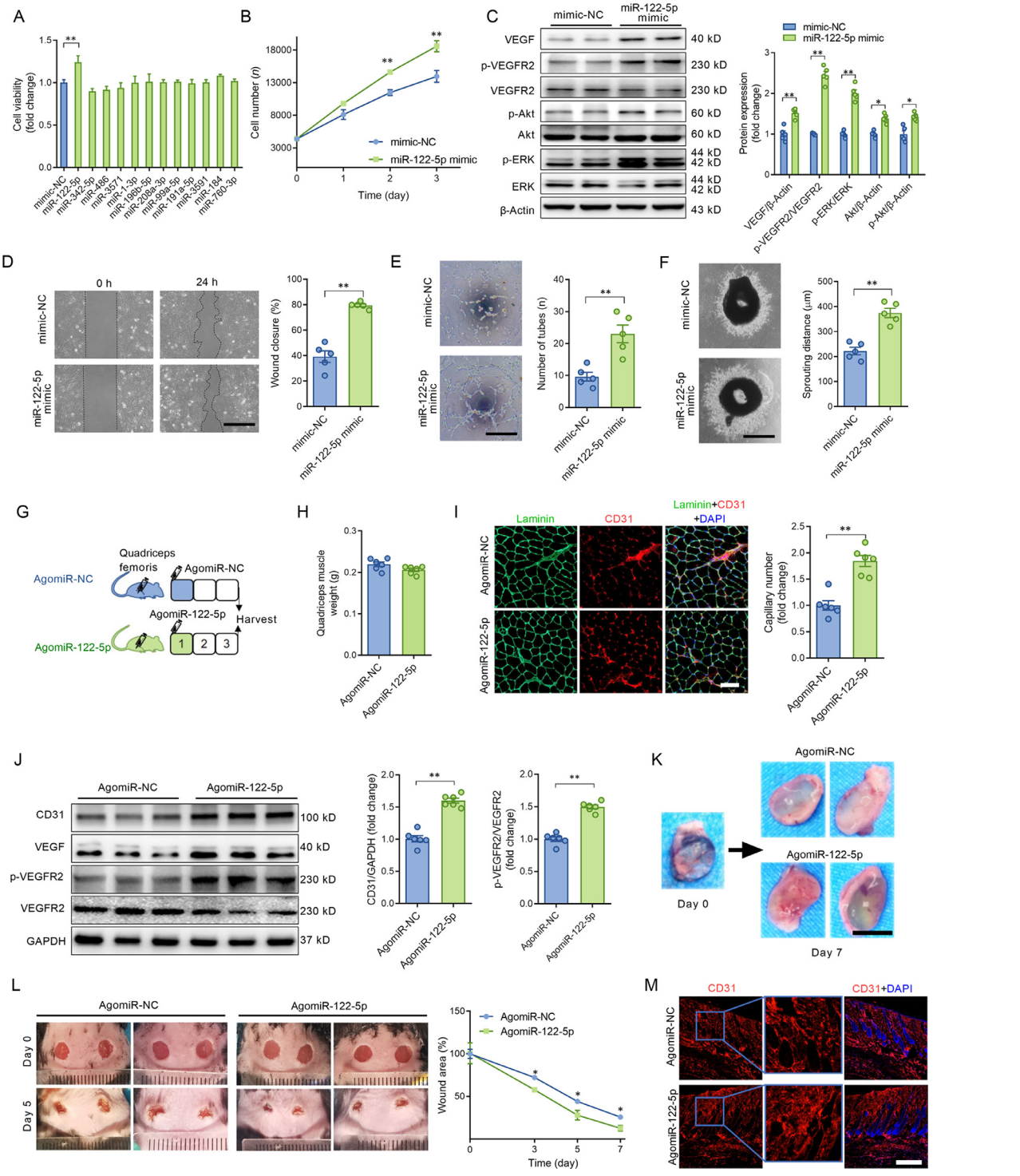

Fig. 1. miR-122-5p stood out as a potent miRNA in the promotion of angiogenesis. (A) The effects of 12 differentially expressed miRNAs mimics on cell viability in ECs; (B) The miR-122-5p mimic increased cell viability in ECs; (C) The miR-122-5p mimic increased the contents of VEGF, p-VEGFR2/VEGFR2, p-ERK/ERK, p-Akt, and Akt in ECs; (D) The miR-122-5p mimic enhanced wound-induced cell migration at 24 h post-wound-formation as detected by the scratch assay in ECs; (E) The miR-122-5p mimic promoted tube-like network formation in ECs; (F) The miR-122-5p mimic increased aortic ring sprouting in cultured aortic rings; (G) Mouse quadriceps muscle was injected with agomiR-NC or agomiR-122-5p to test whether miR-122-5p upregulation promotes angiogenesis in skeletal muscles; (H) Quadriceps muscle weight of mice injected with agomiR-NC or agomiR-122-5p; (I) AgomiR-122-5p increased capillary density in the quadriceps muscle; (J) AgomiR-122-5p increased the contents of CD31, VEGF, and p-VEGFR2 in the quadriceps muscle; (K) AgomiR-122-5p increased the number of newly formed blood vessels in the Matrigel plug; (L) AgomiR-122-5p accelerated wound closure in mice with skin injuries; and (M) AgomiR-122-5p increased capillary density in perilesional skin tissues. Scale bars: 500 μm (D and F); 200 μm (E); 100 μm (I); 1 cm (K); 400 μm (M). $n = 5$ (A–F). $n = 6$ (H–M). Values are presented as mean ± SEM. Data are analyzed using the unpaired Student t test. * $p < 0.05$; ** $p < 0.01$. Akt = protein kinase B; CD31 = platelet/endothelial cell adhesion molecule-1; DAPI = 4',6-diamidino-2-phenylindole; EC = endothelial cell; ERK = extracellular signal-regulated kinase; GAPDH = glyceraldehyde-3-phosphate dehydrogenase; miR = microRNA; NC = negative control; p = phophos; VEGF = vascular endothelial growth factor; VEGFR2 = VEGF receptor-2.

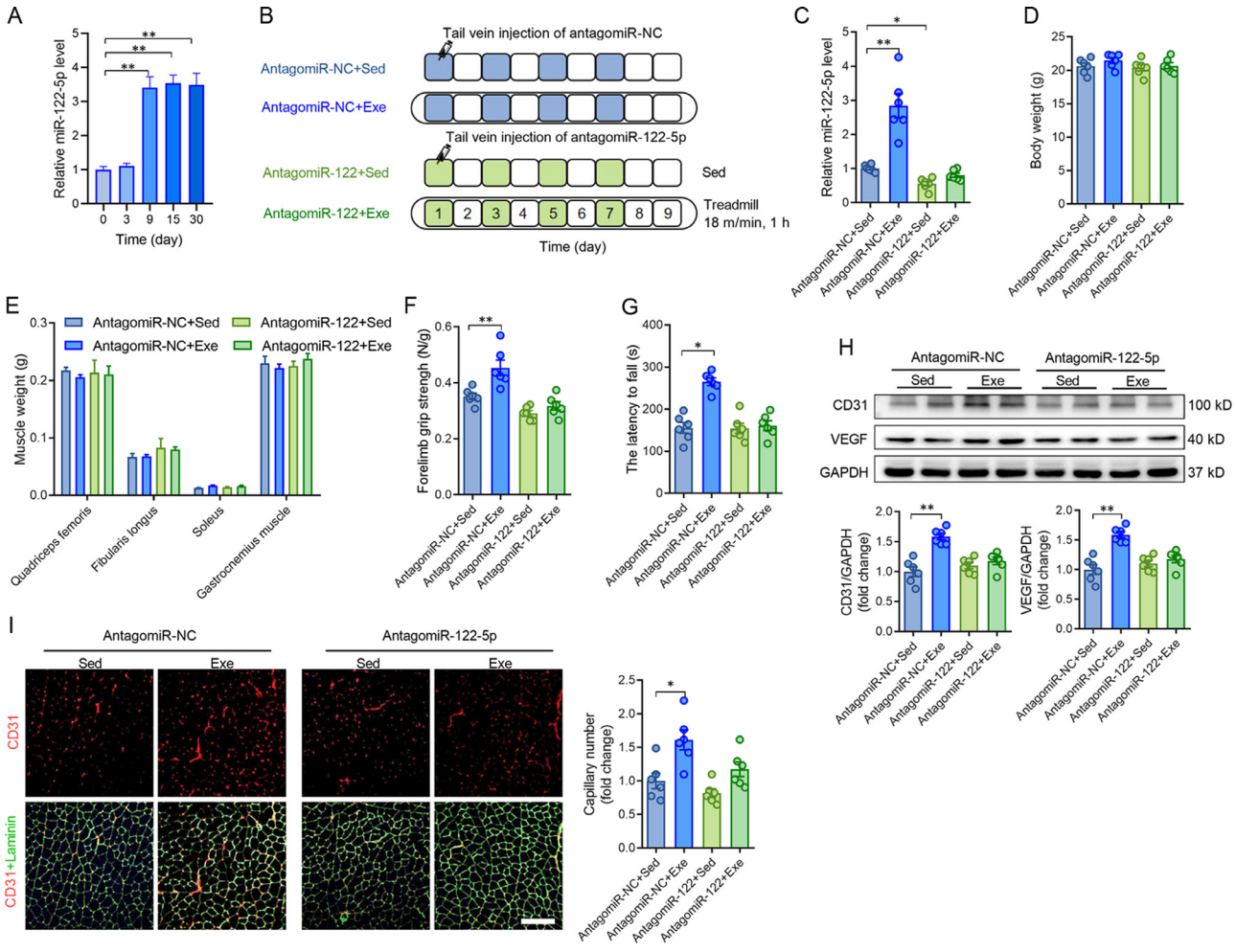

Fig. 2. Exercise promoted angiogenesis through upregulation of circulating miR-122-5p. (A) Circulating miR-122-5p levels in mice following different days of exercise; (B) AntagomiR-122-5p was used to test whether miR-122-5p mediates the exercise-induced angiogenesis in skeletal muscles; (C) AntagomiR-122-5p blocked the upregulation of circulating miR-122-5p induced by exercise; (D and E) AntagomiR-122-5p showed no significant effects on (D) body weight and (E) muscle weight of the mice; (F and G) Exercise-increased muscle performance as detected by (F) forelimb grip strength and (G) rotarod test was abolished by antagomiR-122-5p; (H) Exercise-increased expression levels of CD31 and VEGF; and (I) capillary density in skeletal muscles were abolished by antagomiR-122-5p. Scale bars = 200 μm (I). $n = 6$. Values are presented as mean ± SEM. Data are analyzed using two-way ANOVA followed by unpaired t tests. * $p < 0.05$; ** $p < 0.01$. ANOVA = analysis of variance; CD31 = platelet/endothelial cell adhesion molecule-1; Exe = exercise; GAPDH = glyceraldehyde-3-phosphate dehydrogenase; miR = miRNA; NC = negative control; Sed = sedentary; VEGF = vascular endothelial growth factor.

from sedentary and exercised mice (Fig. 3B and 3C), which is consistent with our previous report.[19] In addition, miR-122-5p was abundant in the extracellular vesicle fraction, and exercise increased miR-122-5p content in the extracellular vesicle fraction, whereas the content of miR-122-5p was very low in the supernatant fraction (extracellular vesicle-free) of the plasma from both exercised and sedentary mice (Fig. 3D), suggesting that circulating miR-122-5p is shuttled mainly by extracellular vesicles. Furthermore, extracellular vesicles isolated from exercised mice increased wound closure and tube-like network formation compared with extracellular vesicles isolated from sedentary mice (Supplementary Fig. 4). In addition, these effects of isolated extracellular vesicles from exercised mice were attenuated by the miR-122-5p inhibitor (Supplementary Fig. 4).

To explore the origins of the circulating miR-122-5p, the expression levels of mature miR-122-5p and its precursor, pre-miR-122-5p, were detected in the liver, skeletal muscle, heart, epididymal fat, kidney, and aorta. As shown in Fig. 3E, miR-122-5p was specifically highly expressed in the liver, and its contents were low in other tissues. Exercise increased the contents of both mature miR-122-5p and pre-miR-122-5p in the liver (Fig. 3E and 3F), suggesting that the liver is a major source of exercise-upregulated miR-122-5p. To test whether liver-derived miR-122-5p plays an important role in exercise-induced angiogenesis, liver-specific knockdown of miR-122-5p by AAV8 carrying antisense miR-122-5p oligomers was used (Fig. 3G). AAV infection downregulated miR-122-5p in the liver, skeletal muscle, heart, and kidney in sedentary mice and blocked the upregulation of miR-122-5p in the liver and skeletal muscle in response to exercise (Fig. 3H). Liver-specific knockdown of miR-122-5p abolished the effects of exercise in the upregulation of miR-122-5p in plasma (Fig. 3I). Liver-specific knockdown of miR-122-5p showed no significant effects on body weight and muscle mass in mice

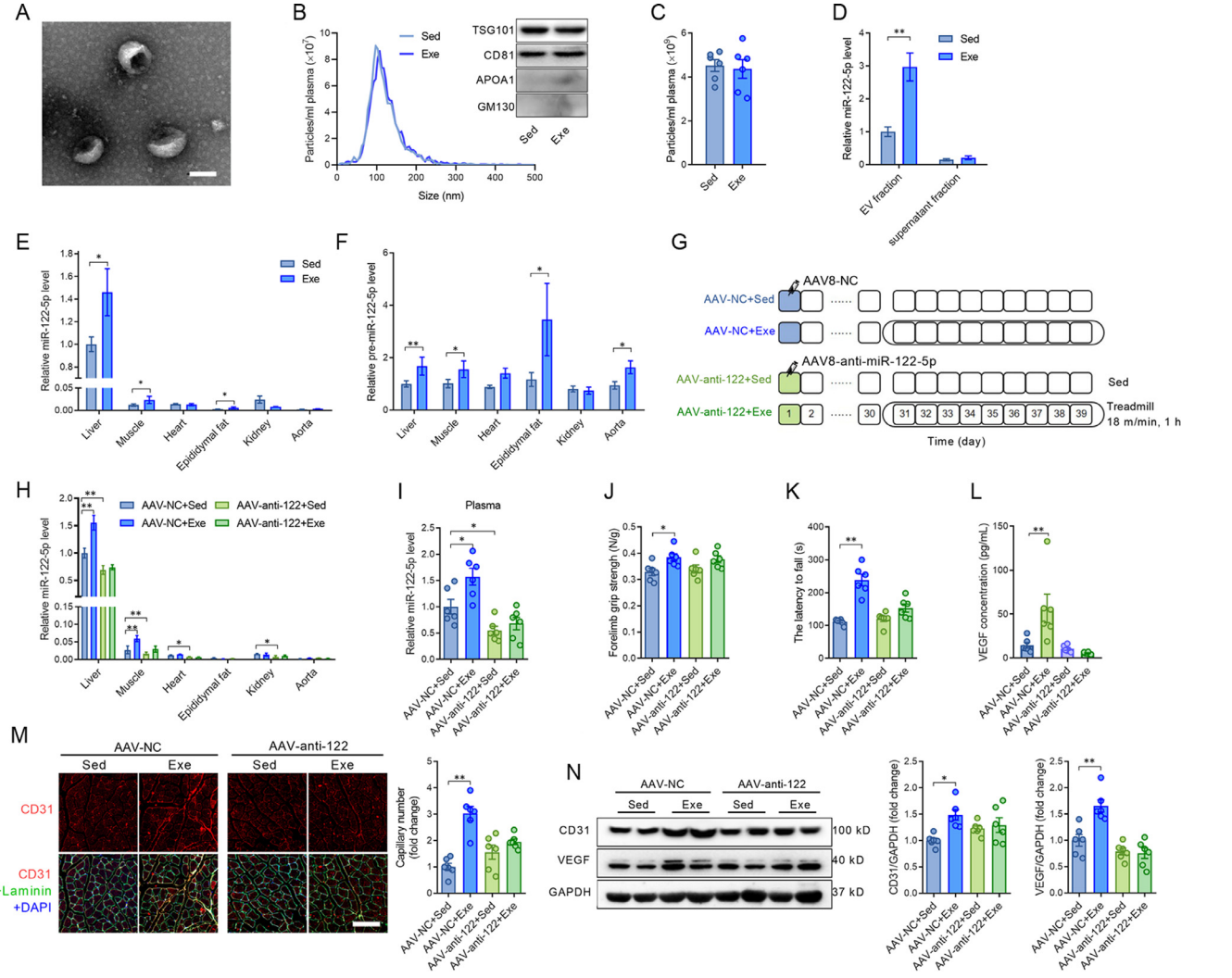

Fig. 3. Exercise-upregulated miR-122-5p was shuttled by extracellular vesicles and derived from the liver. (A) Electron microscopy analysis revealed typical rounded particles (extracellular vesicle, EV) in isolated fractions; (B) Nanoparticle tracking analysis and Western blot analysis of extracellular vesicles isolated from sedentary and exercised mice; (C) Particle concentration in plasma from sedentary and exercised mice; (D) Contents of miR-122-5p in the extracellular vesicle fraction and the supernatant fraction (extracellular vesicle free) isolated from plasma of sedentary and exercised mice; (E) Expression profile of miR-122-5p in different tissues in response to exercise; (F) Expression profile of pre-miR-122-5p in different tissues in response to exercise; (G) Liver-specific knockdown of miR-122-5p by AAV8 carrying antisense miR-122-5p oligomers was used to test whether liver-derived miR-122-5p contributes to exercise-induced angiogenesis; (H) AAV infection downregulated miR-122-5p in the liver, skeletal muscle, heart, and kidney in sedentary mice and blocked the upregulation of miR-122-5p in the liver and skeletal muscle in response to exercise; (I) Liver-specific knockdown of miR-122-5p abolished the effects of exercise in upregulation of miR-122-5p in plasma; (J and K) Liver-specific knockdown of miR-122-5p abolished the effects of exercise in promotion of muscle performance as detected by (J) forelimb grip strength and (K) motor coordination; (L) AAV-anti-122 blocked the upregulation of serum VEGF concentration induced by exercise; (M and N) Liver-specific knockdown of miR-122-5p abolished the effects of exercise in promotion of angiogenesis as detected by (M) CD31 staining and (N) expression levels of CD31 and VEGF in skeletal muscles. Scale bars: 100 nm (A); 100 μm (M). $n = 6$. Values are presented as mean ± SEM. Data are analyzed using the unpaired Student t test (C–F,) and two-way ANOVA followed by unpaired t tests (H–N). * $p < 0.05$; ** $p < 0.01$. AAV = adeno-associated virus; ANOVA = analysis of variance; APOA1 = apolipoprotein A1; CD31 = platelet/endothelial cell adhesion molecule-1; DAPI = 4',6-diamidino-2-phenylindole; Exe = exercise; GM130 = golgi matrix protein 130; NC = negative control; Sed = sedentary; TSG101 = tumor susceptibility 101; VEGF = vascular endothelial growth factor.

(Supplementary Fig. 5) but abolished the effects of exercise in promotion of muscle performance as evidenced by forelimb grip strength and motor coordination (Fig. 3J and 3K). Liver-specific knockdown of miR-122-5p abolished the effects of exercise in the promotion of angiogenesis as detected by capillary density and expression levels of CD31 and VEGF in skeletal muscles and upregulation of circulating VEGF (Fig. 3L–3N). In addition, extracellular vesicles isolated from the liver were more easily taken up by cultured ECs (Supplementary Fig. 6). Furthermore, inhibition of extracellular vesicle secretion using GW4869 (S7609; Selleck, Houston, TX, USA) attenuated the upregulation of circulating miR-122-5p and the expression levels of CD31 and capillary density in skeletal muscles in exercised mice (Supplementary Fig. 7). These results suggest that exercise promotes angiogenesis through extracellular vesicle-shuttled and liver-derived miR-122-5p in skeletal muscles.

3.4. miR-122-5p promoted angiogenesis through enhancing fatty acid utilization in ECs

Target genes of miR-122-5p were predicted by miRanda, miRDB, and TargetScan. These genes were functionally classified by the DAVID gene functional classification tool. Among the possible miR-122-5p target genes, 6 genes were negative regulators of angiogenesis (Fig. 4A). None of these genes were decreased by the miR-122-5p mimic (Fig. 4B), suggesting that miR-122-5p is not likely to promote angiogenesis by directly targeting negative regulators of angiogenesis. Recent studies have shown that angiogenesis is regulated by metabolic shift in ECs.[22,23] Thus, we next tested the role of miR-122-5p in the regulation of substrate preference in cultured ECs. As shown in Fig. 4C and 4D, the miR-122-5p mimic increased fatty acids uptake but showed no significant effects on glucose uptake. In addition, the miR-122-5p mimic increased expression levels of CD36 and CPT1A (Fig. 4E) and increased fatty acid oxidation in ECs (Fig. 4F and 4G), suggesting that miR-122-5p promotes fatty acid utilization in ECs. Next, CD36 was knocked down using siRNA to test whether fatty acid utilization is involved in miR-122-5p-induced angiogenesis. CD36 knockdown showed no significant effects on VEGF, p-VEGFR2/VEGFR2, p-Akt, and Akt contents but decreased p-ERK/ERK content in ECs without miR-122-5p transfection (Fig. 4H). CD36 knockdown abolished the effects of the miR-122-5p mimic on upregulation of VEGF, p-VEGFR2/VEGFR2, Akt, p-Akt, and p-ERK/ERK contents in ECs (Fig. 4H). CD36 knockdown decreased the effects of the miR-122-5p mimic on the promotion of wound closure as detected by scratch assay (Fig. 4I). In addition, CD36 knockdown decreased the effects of the miR-122-5p mimic on promoting tube-like network formation and aortic ring sprouting (Fig. 4J and 4K). These results suggest that miR-122-5p promotion of angiogenesis is dependent on fatty acid utilization.

In fact, we observed that CPT1A and CD36 were highly expressed in ECs in skeletal muscles, as detected by immunofluorescence (Supplementary Fig. 8). AgomiR-122-5p increased CD36 and CPT1A expression levels in ECs in quadriceps muscles (Supplementary Fig. 8). Exercise increased CD36 and CPT1A expression levels in ECs in skeletal muscles, which was abolished by antagomiR-122-5p treatment (Supplementary Fig. 8). Detection of the levels of circulating lipids revealed that neither antagomiR-122-5p nor exercise showed any significant effects on circulating levels of lipids (Supplementary Fig. 9). These results suggest that exercise and miR-122-5p upregulate fatty acid utilization in ECs in skeletal muscles.

3.5. miR-122-5p promoted angiogenesis through targeting AGPAT1

Among the possible miR-122-5p target genes, 6 genes were negative regulators of fatty acids metabolism (Fig. 5A). The miR-122-5p mimic downregulated *Agpat1* expression, and miR-122-5p inhibitor upregulated *Agpat1* expression in both mRNA level and protein level (Fig. 5B–5D), suggesting that *Agpat1* is a potential target of miR-122-5p. The binding sites for miR-122-5p in the 3'-untranslated regions (3'UTRs) of *Agpat1* were further examined using a luciferase reporter assay (Supplementary Fig. 10). The results showed that miR-122-5p reduced luciferase activity for *Agpat1* wild-type 3′UTR constructs but had no effects when the miR-122-5p binding sites were mutated (Fig. 5E). Knockdown of AGPAT1 increased fatty acid utilization, as evidenced by increased expression levels of CD36 and CPT1A, and increased fatty acid oxidation in ECs (Fig. 5F–5H). Knockdown of AGPAT1 abolished the effects of the miR-122-5p mimic on upregulation of fatty acid utilization (Fig. 5F–5H). Knockdown of AGPAT1 increased the expression of VEGF and phosphorylation of VEGFR2, and abolished the effects of miR-122-5p on upregulation of VEGF and p-VEGFR2 in cultured ECs (Fig. 5H). Knockdown of AGPAT1 showed no significant effects on tube-like network formation, but it increased cell migration and aortic ring sprouting (Fig. 5I–5K). Knockdown of AGPAT1 abolished the effects of the miR-122-5p mimic on promotion of migration, tube-like network formation and aortic ring sprouting (Fig. 5I–5K). These results suggest that miR-122-5p promotes angiogenesis through targeting AGPAT1.

The immunofluorescence assay showed that AGPAT1 was abundantly expressed in ECs in quadriceps muscles (Fig. 6A). AgomiR-122-5p downregulated AGPAT1 expression in ECs in quadriceps muscles (Fig. 6A). Western blot analysis confirmed the decreased expression of AGPAT1 in skeletal muscles with agomiR-122-5p treatment (Fig. 6B). Exercise decreased AGPAT1 expression, and antagomiR-122-5p abolished the effects of exercise on downregulation of AGPAT1 in ECs in skeletal muscles (Fig. 6C). Western blot analysis confirmed the decreased expression of AGPAT1 in skeletal muscles from exercised mice, and antagomiR-122-5p abolished the effects of exercise on downregulation of AGPAT1 in skeletal muscles (Fig. 6D). In addition, the protein expression levels were also detected by western blot in perilesional skin samples from agomiR-NC- and agomiR-122-5p-treated mice with wounds. AgomiR-122-5p treatment increased the contents of CD31, VEGF, p-VEGFR2, CD36, and CPT1A and decreased the expression of AGPAT1 in perilesional skin tissues (Fig. 6E). These results reinforce the notion that miR-122-5p promotes angiogenesis through targeting AGPAT1 in ECs.

4. Discussion

We previously identified a cluster of differentially expressed exosomal miRNAs after exercise and found that some of them act as cardioprotective exerkines.[19] In the present study, we found extracellular vesicle miR-122-5p as a new exerkine in the promotion of angiogenesis. miR-122-5p is derived mainly from the liver and enhances fatty acid utilization by targeting AGPAT1 in ECs, leading to new primary capillary formation (Fig. 6F). Our findings reveal a novel mechanism in that exercise shifts endothelial substrate preference and promotes angiogenesis via liver-derived extracellular vesicle miR-122-5p. Our findings also highlight the therapeutic potential of extracellular vesicle exerkine.

The increase in muscle vascularization is significant at an early stage postexercise, leading to a ~5-fold increase in blood flow and a 20% increase in capillary density even after several

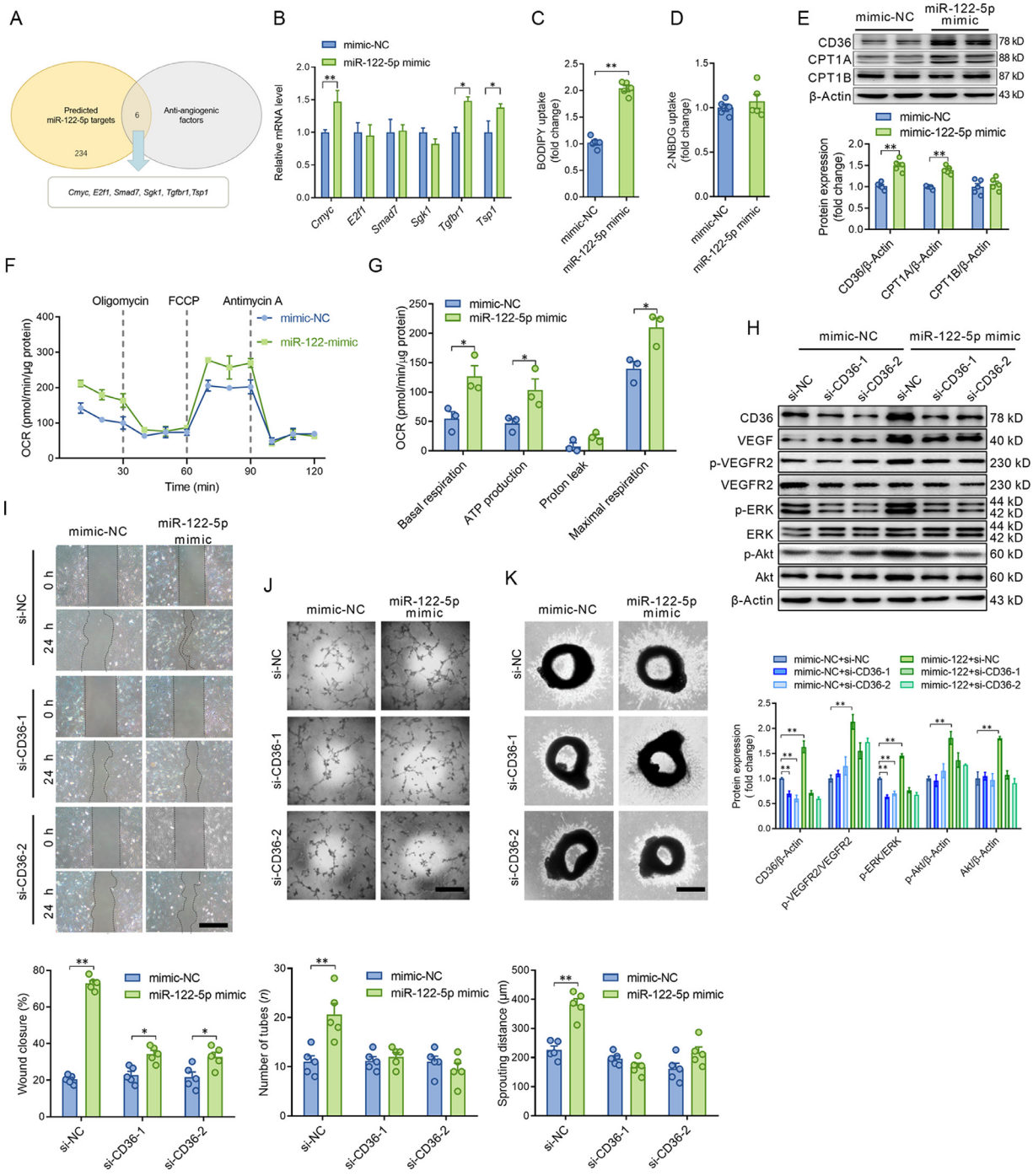

Fig. 4. miR-122-5p promoted angiogenesis through enhancing fatty acid utilization in ECs. (A) Target genes of miR-122-5p were predicted by miRanda, miRDB, and TargetScan. Among the possible miR-122-5p target genes, 6 genes were negative regulators of angiogenesis; (B) Expression levels of the predicted negative regulators of angiogenesis from (A) were detected in ECs transfected with NC or the miR-122-5p mimic; (C and D) The miR-122-5p mimic (C) increased fatty acids uptake and (D) showed no significant effect on glucose uptake; (E) The miR-122-5p mimic increased the expression levels of CD36 and CPT1A in cultured ECs; (F and G) The miR-122-5p mimic increased fatty acid oxidation in ECs as detected by seahorse. Only palmitic acid (PA) was provided in the detection medium. Oligomycin, FCCP, and antimycin A act as ATP synthase inhibitor, mitochondrial uncoupler, and complex III inhibitor, respectively; (H) CD36 knockdown abolished the effects of the miR-122-5p mimic on upregulation of VEGF, p-VEGFR2/VEGFR2, p-Akt, Akt, and p-ERK/ERK contents in ECs; (I) CD36 knockdown decreased the effects of the miR-122-5p mimic on the promotion of wound closure as detected by scratch assay; (J and K) CD36 knockdown decreased the effects of the miR-122-5p mimic on (J) promoting tube-like network formation in ECs and (K) aortic ring sprouting in cultured aortic rings. Scale bars: 500 μm (I and K); 200 μm (J). $n = 3$ in (F) and (G) and $n = 5$ in other figures. Values are presented as mean ± SEM. Data are analyzed using the unpaired Student *t* test in (B−G) and two-way ANOVA followed by unpaired *t* tests in H−K. * $p < 0.05$; ** $p < 0.01$. 2-NBDG = 2-(N-(7-nitrobenz-2-oxa-1,3-diaxol-4-yl) amino)-2-deoxyglucose; Akt = protein kinase B; ANOVA = analysis of variance; CD36 = fatty acid translocase; *Cmyc* = cellular myelocytomatosis oncogene; CPT1 = carnitine palmitoyl-transferase 1; *E2f1* = E2F transcription factor 1; EC = endothelial cell; ERK = extracellular signal-regulated kinase; FCCP = carbonilcyanide p-triflouromethoxyphenylhydrazone; miR = miRNA; NC = negative control; OCR = oxygen consumption rate; *Sgk1* = serum/glucocorticoid regulated kinase 1; si = small interference; *Smad7* = SMAD family member 7; *Tgfbr1* = transforming growth factor β receptor 1; *Tsp1* = thrombospondin-1; VEGF = vascular endothelial growth factor; VEGFR2 = VEGF receptor-2.

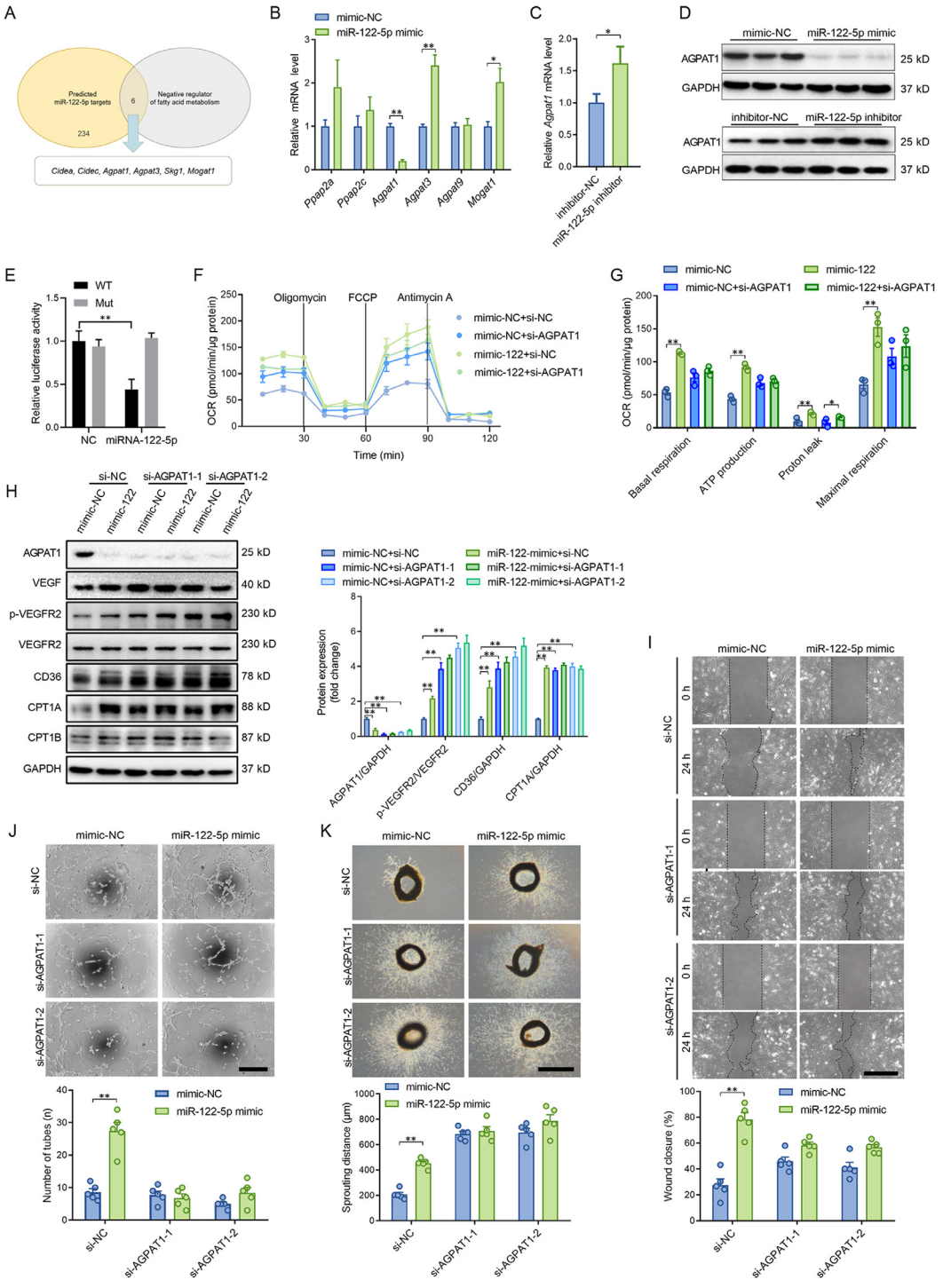

Fig. 5. miR-122-5p promoted angiogenesis through targeting AGPAT1. (A) Among the possible miR-122-5p target genes, 6 genes were negative regulators of fatty acids metabolism; (B) The miR-122-5p mimic downregulated *Agpat1* expression; (C) The miR-122-5p inhibitor upregulated *Agpat1* expression; (D) The miR-122-5p mimic downregulated AGPAT1 expression and the miR-122-5p inhibitor upregulated AGPAT1 expression at the protein level; (E) miR-122-5p reduced luciferase activity for *Agapt1* wild-type 3'UTR constructs but had no effect when the miR-122-5p binding sites were mutated; (F and G) Knockdown of AGPAT1 increased fatty acid utilization and blocked the effects of miR-122-5p on upregulation of fatty acid oxidation; (H) Knockdown of AGPAT1 abolished the effects of miR-122-5p on upregulation of VEGF, p-VEGFR2, CD36, and CPT1A in cultured ECs. (I and K) Knockdown of AGPAT1 abolished the effects of the miR-122-5p mimic on (I) promotion of migration, (J) tube-like network formation, and (K) aortic ring sprouting. Scale bars: 500 μm (I and K); 200 μm (J). $n = 3$ in (F and G) and $n = 5$ in (B-E) and (H and I). Values are presented as mean ± SEM. Data are analyzed using the unpaired Student *t* test in (B and C) and two-way ANOVA followed by unpaired *t* tests in (E−K). * $p < 0.05$; ** $p < 0.01$. *Agpat* = 1-acyl-sn-glycerol-3-phosphate acyltransferase; ANOVA = analysis of variance; CD36 = fatty acid translocase; *Cidea,c* = cell death inducing DFFA like effector a,c; CPT1 = carnitine palmitoyl-transferase 1; FCCP = carbonilcyanide p-triflouromethoxyphenylhydrazone; GAPDH = glyceraldehyde-3-phosphate dehydrogenase; miR = microRNA; *Mogat1* = monoacylglycerol O-acyltransferase; Mut = mutant; NC = negative control; OCR = oxygen consumption rate; *Ppap2a, c* = phosphatidic acid phosphatase type 2a, c; p-VEGFR2 = phospho-VEGF receptor-2; UTR = untranslated region; VEGF = vascular endothelial growth factor; WT = wild type.

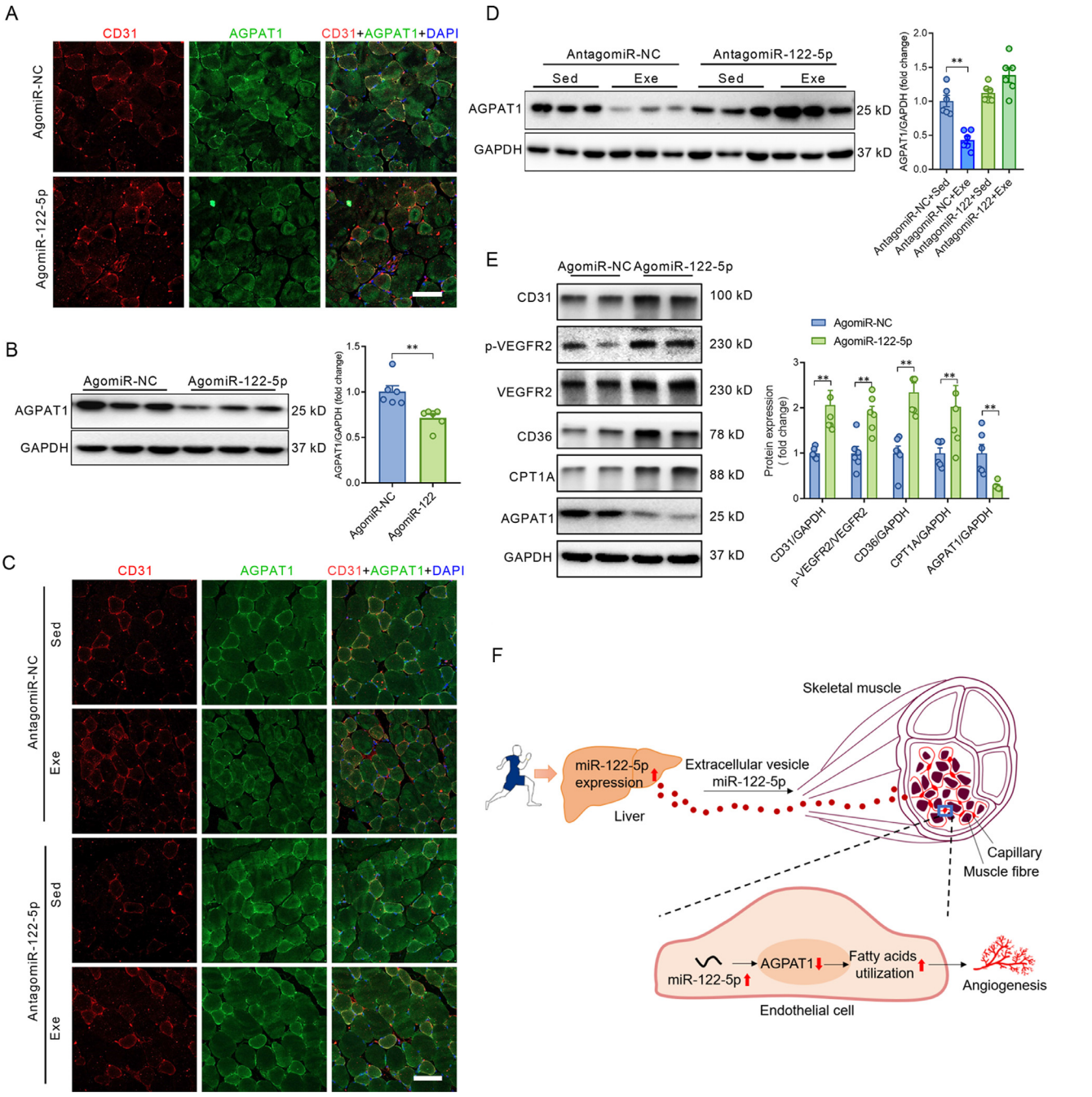

Fig. 6. miR-122-5p downregulated AGPAT1 expression in ECs *in vivo*. (A) AgomiR-122-5p downregulated AGPAT1 expression in ECs, as detected by immunofluorescence in skeletal muscles injected with either agomiR-NC or agomiR-122-5p; (B) Western blot analysis confirmed the decreased expression of AGPAT1 in skeletal muscles with agomiR-122-5p treatment; (C) Exercise decreased AGPAT1 expression, and antagomiR-122-5p abolished the effects of exercise on downregulation of AGPAT1 in ECs in skeletal muscles; (D) Western blot analysis confirmed the decreased expression of AGPAT1 in skeletal muscles in exercised mice, and antagomiR-122-5p abolished the effects of exercise on downregulation of AGPAT1 in skeletal muscles; (E) Protein expressions in perilesional skin samples from mice with skin wound; and (F) Graphic summary of the findings. Scale bars: 100 μm (A and C). $n = 6$. Values are presented as mean ± SEM. Data are analyzed using the unpaired Student *t* test in (B and E) and two-way ANOVA followed by unpaired *t* tests in (D). * $p < 0.05$; ** $p < 0.01$. AGPAT1 = 1-acyl-sn-glycerol-3-phosphate acyltransferase; ANOVA = analysis of variance; CD31 = platelet/endothelial cell adhesion molecule-1; CD36 = fatty acid translocase; CPT1A = carnitine palmitoyl-transferase 1A; DAPI = 4',6-diamidino-2-phenylindole; Exe = exercise; GAPDH = glyceraldehyde-3-phosphate dehydrogenase; NC = negative control; p = phosphorylation; Sed = sedentary; VEGFR2 = vascular endothelial growth factor receptor-2.

days of training.[6,7] It has been reported that an increase in muscle capillarity plays a critical role in the beneficial effects of exercise in improving muscle mass and performance, which improves blood/tissue exchange by increasing oxygen diffusion, thus promoting nutrient consumption and enhancing clearance of toxic waste products.[22] The growth of functional capillaries following exercise is the result of increases in pro-angiogenic factors, among which VEGF signaling plays a crucial role. Even acute exercise bouts increased VEGF mRNA and protein levels transiently in skeletal muscles.[24–26] Several

intracellular factors are reported to be involved in exercise-induced angiogenesis, including the estrogen-related receptor γ, peroxisome-proliferator-activated receptor-γ coactivator-1α, 5' adenosine monophosphate-activated protein kinase, and hypoxia-inducible factor 1α.[22] Recent studies support the notion that exercise-induced bioactive factors (exerkines) released into circulation, including proteins, peptides, nucleic acids, other molecules secreted from skeletal muscles, adipose tissue (adipokine), and many other tissues, have been implicated in the beneficial effects of exercise.[1] Exerkines, including interleukin-6 (IL-6), IL-7, IL-8, hepatocyte growth factor, reactive oxygen species, angiopoietin 1, and angiopoietin 2, have been reported to contribute to exercise-promoted angiogenesis.[1]

Recently, there has been a growing focus on extracellular vesicle-mediated cell-to-cell communication.[27–29] Extracellular vesicles are believed to harbor exerkines and deliver them through systemic circulation.[17,18] We found previously that aerobic exercise-derived circulating extracellular vesicles afford profound and sustained cardioprotection against myocardial ischemia/reperfusion, even though their plasma concentration provides no significant change.[19] Exercise changed the profile of exosomal miRNAs in circulation, and we believe that these exercise-regulated miRNAs have a different biological significance. Exosomal miR-342-5p was identified as a key exerkine that mediates the cardioprotective effects of exercise.[19] In the present study, we found that miR-122-5p derived from the liver plays an important role in promoting angiogenesis in both skeletal muscles and injured tissues, indicating a crosstalk between the liver and ECs in response to exercise. miR-122-5p activated VEGF signaling by phosphorylation of VEGFR2 and enhancement of VEGF expression and secretion in ECs. Previous studies have also identified other exerkines derived from the liver (hepatokines), including fibroblast growth factor 21 and glycosylphosphatidylinositol-specific phospholipase D1,[30,31] both of which are closely associated with metabolic regulation,[32,33] suggesting that the liver is an essential organ in the regulation of metabolism in other cells. miR-122-5p, which accounts for 70% of the liver's total miRNAs,[34] has been extensively studied. These previous studies have shown that miR-122-5p plays a critical role in liver homeostasis, including cholesterol and free fatty acid metabolism,[35] hepatocellular carcinoma growth,[36] hepatitis C virus replication,[37] and hepatic circadian regulation.[38] Circulating miR-122-5p was found to be involved in the regulation of erythropoietin production in the kidney,[39] in cancer,[40] in systemic iron homeostasis,[41] and in virus-induced lung disease.[42] The present study extends these findings, showing that miR-122-5p facilitates exercise-improved angiogenesis as an exerkine, which contributes to the improvement of muscle mass and function as well as tissue repair.

ECs are highly glycolytic, producing 85% of their energy through glycolysis even under well-oxygenated conditions.[43] They upregulate glycolysis even further when they sprout into avascular areas.[43–45] Although mitochondrial bioenergetics contributes to low adenosine triphosphate production in ECs, evidence has shown that mitochondria play important role in angiogenesis.[46] For example, it has been reported that fatty acid oxidation is required for nucleotide synthesis and that blocking fatty acid utilization impairs EC proliferation.[47] In addition, it has been shown that intermediates of lipid synthesis regulate EC proliferation through post-translational modification of the mechanistic target of rapamycin complex 1.[48] These advances suggest that angiogenesis is tightly regulated by metabolism. In the present study, we found that miR-122-5p enhances fatty acid utilization, and its role in the promotion of angiogenesis is dependent on its effects in enhancing fatty acid utilization. In fact, it has been reported that miR-122-5p plays a role in the promotion of cholesterol and free fatty acid metabolism and that the level of promotion is associated with the risk of new-onset metabolic syndrome and type 2 diabetes.[49] Therefore, we tested whether miR-122-5p regulates angiogenesis through the regulation of fatty acid metabolism and found that miR-122-5p promotes angiogenesis through targeting AGPAT1. AGPAT1 is an enzyme that converts lysophosphatidic acid into phosphatidic acid, the initial step in glycerolipid synthesis. Evidence has shown that knockout of AGPAT1 increases fatty acid oxidation,[50] which is consistent with our results. Our results also show that AGPAT1 and CPT1A are abundantly expressed in ECs, reinforcing the important role of fatty acid utilization in the regulation of endothelial function.

5. Conclusion

Taken together, these findings suggest that exercise promotes angiogenesis through upregulation of extracellular vesicle miR-122-5p. Extracellular vesicle miR-122-5p is derived mainly from the liver and promotes new primary capillary formation through targeting AGPAT1, which shifts substrate preference to fatty acids in ECs. Our findings represent a novel mechanism underlying exercise-afforded angiogenesis, with extracellular vesicle miR-122-5p as a novel exerkine, thus highlighting its therapeutic potential in tissue repair.

Acknowledgments

This work was supported by the National Key Basic Research Program of China (2019YFF0301600 and 2020YFC2002900), National Natural Science Foundation of China (31930055, 31871146, 32071169, 81870273, and 32071108), and Major Basic Science Program of Shaanxi Provincial Natural Science Foundation of China (2016ZDJC-17).

Authors' contributions

XZ, LZ, and FG conceived and supervised the study and wrote the manuscript; JLou, JW, MF, XD, GW, HY, YW, and YZ performed the experiments and analyzed the data; JLi, CS, and JLiu conceived the study. All authors have read and approved the final version of the manuscript, and agree with the order of presentation of the authors.

Competing interests

The authors declare that they have no competing interests.

Supplementary materials

Supplementary materials associated with this article can be found in the online version at doi:10.1016/j.jshs.2021.09.009.

References

1. Fiuza-Luces C, Garatachea N, Berger NA, Lucia A. Exercise is the real polypill. *Physiology (Bethesda)* 2013;**28**:330–58.
2. Li S, Laher I. Exercise pills: At the starting line. *Trends Pharmacol Sci* 2015;**36**:906–17.
3. Luan X, Tian X, Zhang H, et al. Exercise as a prescription for patients with various diseases. *J Sport Health Sci* 2019;**8**:422–41.
4. Laufs U, Werner N, Link A, et al. Physical training increases endothelial progenitor cells, inhibits neointima formation, and enhances angiogenesis. *Circulation* 2004;**109**:220–6.
5. Bloor CM. Angiogenesis during exercise and training. *Angiogenesis* 2005;**8**:263–71.
6. Hudlicka O, Brown MD. Adaptation of skeletal muscle microvasculature to increased or decreased blood flow: Role of shear stress, nitric oxide and vascular endothelial growth factor. *J Vasc Res* 2009;**46**:504–12.
7. Waters RE, Rotevatn S, Li P, Annex BH, Yan Z. Voluntary running induces fiber type-specific angiogenesis in mouse skeletal muscle. *Am J Physiol Cell Physiol* 2004;**287**:C1342–8.
8. Potente M, Gerhardt H, Carmeliet P. Basic and therapeutic aspects of angiogenesis. *Cell* 2011;**146**:873–87.
9. Van Craenenbroeck EM, Hoymans VY, Beckers PJ, et al. Exercise training improves function of circulating angiogenic cells in patients with chronic heart failure. *Basic Res Cardiol* 2010;**105**:665–76.
10. Falanga V. Wound healing and its impairment in the diabetic foot. *The Lancet* 2005;**366**:1736–43.
11. Inampudi C, Akintoye E, Ando T, Briasoulis A. Angiogenesis in peripheral arterial disease. *Curr Opin Pharmacol* 2018;**39**:60–7.
12. Hawley JA, Hargreaves M, Joyner MJ, Zierath JR. Integrative biology of exercise. *Cell* 2014;**159**:738–49.
13. Safdar A, Saleem A, Tarnopolsky MA. The potential of endurance exercise-derived exosomes to treat metabolic diseases. *Nat Rev Endocrinol* 2016;**12**:504–17.
14. Wu G, Zhang X, Gao F. The epigenetic landscape of exercise in cardiac health and disease. *J Sport Health Sci* 2021;**10**:648–59.
15. Pedersen BK. Anti-inflammatory effects of exercise: Role in diabetes and cardiovascular disease. *Eur J Clin Invest* 2017;**47**:600–11.
16. Lecker SH, Zavin A, Cao P, et al. Expression of the irisin precursor FNDC5 in skeletal muscle correlates with aerobic exercise performance in patients with heart failure. *Circ Heart Fail* 2012;**5**:812–8.
17. Whitham M, Parker BL, Friedrichsen M, et al. Extracellular vesicles provide a means for tissue crosstalk during exercise. *Cell Metab* 2018;**27**:237–51.
18. Trovato E, Di Felice V, Barone R. Extracellular vesicles: Delivery vehicles of myokines. *Front Physiol* 2019;**10**:522. doi:10.3389/fphys.2019.00522.
19. Hou Z, Qin X, Hu Y, et al. Longterm exercise-derived exosomal miR-342-5p: A novel exerkine for cardioprotection. *Circ Res* 2019;**124**:1386–400.
20. Kastana P, Zahra FT, Ntenekou D, et al. Matrigel plug assay for *in vivo* evaluation of angiogenesis. *Methods Mol Biol* 2019;**1952**:219–32.
21. Baker M, Robinson SD, Lechertier T, et al. Use of the mouse aortic ring assay to study angiogenesis. *Nat Protoc* 2011;**7**:89–104.
22. Gorski T, De Bock K. Metabolic regulation of exercise-induced angiogenesis. *Vasc Biol* 2019;**1**:H1–8.
23. Eelen G, de Zeeuw P, Treps L, Harjes U, Wong BW, Carmeliet P. Endothelial cell metabolism. *Physiol Rev* 2018;**98**:3–58.
24. Breen EC, Johnson EC, Wagner H, Tseng HM, Sung LA, Wagner PD. Angiogenic growth factor mRNA responses in muscle to a single bout of exercise. *J Appl Physiol (1985)* 1996;**81**:355–61.
25. Olenich SA, Gutierrez-Reed N, Audet GN, Olfert IM. Temporal response of positive and negative regulators in response to acute and chronic exercise training in mice. *J Physiol* 2013;**591**:5157–69.
26. Olfert IM, Howlett RA, Wagner PD, Breen EC. Myocyte vascular endothelial growth factor is required for exercise-induced skeletal muscle angiogenesis. *Am J Physiol Regul Integr Comp Physiol* 2010;**299**:R1059–67.
27. Thomou T, Mori MA, Dreyfuss JM, et al. Adipose-derived circulating miRNAs regulate gene expression in other tissues. *Nature* 2017;**542**:450–5.
28. Ying W, Riopel M, Bandyopadhyay G, et al. Adipose tissue macrophage-derived exosomal miRNAs can modulate *in vivo* and *in vitro* insulin sensitivity. *Cell* 2017;**171**:372–84.
29. Davidson SM, Andreadou I, Barile L, et al. Circulating blood cells and extracellular vesicles in acute cardioprotection. *Cardiovasc Res* 2019;**115**:1156–66.
30. Horowitz AM, Fan X, Bieri G, et al. Blood factors transfer beneficial effects of exercise on neurogenesis and cognition to the aged brain. *Science* 2020;**369**:167–73.
31. Gonzalez-Gil AM, Elizondo-Montemayor L. The role of exercise in the interplay between myokines, hepatokines, osteokines, adipokines, and modulation of inflammation for energy substrate redistribution and fat mass loss: A review. *Nutrients* 2020;**12**:1899. doi:10.3390/nu12061899.
32. Abdolmaleki F, Heidarianpour A. Endurance exercise training restores diabetes-induced alteration in circulating Glycosylphosphatidylinositol-specific phospholipase D levels in rats. *Diabetol Metab Syndr* 2020;**12**:43. doi:10.1186/s13098-020-00553-z.
33. Wang XP, Xing CY, Zhang JX, et al. Time-restricted feeding alleviates cardiac dysfunction induced by simulated microgravity via restoring cardiac FGF21 signaling. *FASEB J* 2020;**34**:15180–96.
34. Lagos-Quintana M, Rauhut R, Yalcin A, Meyer J, Lendeckel W, Tuschl T. Identification of tissue-specific microRNAs from mouse. *Curr Biol* 2002;**12**:735–9.
35. Krützfeldt J, Rajewsky N, Braich R, et al. Silencing of microRNAs *in vivo* with "antagomirs". *Nature* 2005;**438**:685–9.
36. Tsai WC, Hsu PW, Lai TC, et al. MicroRNA-122, a tumor suppressor microRNA that regulates intrahepatic metastasis of hepatocellular carcinoma. *Hepatology* 2009;**49**:1571–82.
37. Jopling CL, Schütz S, Sarnow P. Position-dependent function for a tandem microRNA miR-122-binding site located in the hepatitis Cvirus RNA genome. *Cell Host Microbe* 2008;**4**:77–85.
38. Gatfield D, Le Martelot G, Vejnar CE, et al. Integration of microRNA miR-122 in hepatic circadian gene expression. *Genes Dev* 2009;**23**:1313–26.
39. Rivkin M, Simerzin A, Zorde-Khvalevsky E, et al. Inflammation-induced expression and secretion of microRNA 122 leads to reduced blood levels of kidney-derived erythropoietin and anemia. *Gastroenterology* 2016;**151**:999–1010.
40. Mei J, Liu G, Wang W, et al. OIP5-AS1 modulates epigenetic regulator HDAC7 to enhance non-small cell lung cancer metastasis via miR-140-5p. *Oncol Lett* 2020;**20**:7. doi:10.3892/ol.2020.11868.
41. Castoldi M, Vujic Spasic M, Altamura S, et al. The liver-specific microRNA miR-122 controls systemic iron homeostasis in mice. *J Clin Invest* 2011;**121**:1386–96.
42. Collison AM, Sokulsky LA, Kepreotes E, et al. miR-122 promotes virus-induced lung disease by targeting SOCS1. *JCI Insight* 2021;**6**:e127933. doi:10.1172/jci.insight.127933.
43. De Bock K, Georgiadou M, Schoors S, et al. Role of PFKFB3-driven glycolysis in vessel sprouting. *Cell* 2013;**154**:651–63.
44. Schoors S, De Bock K, Cantelmo AR, et al. Partial and transient reduction of glycolysis by PFKFB3 blockade reduces pathological angiogenesis. *Cell Metab* 2014;**19**:37–48.
45. Yu P, Wilhelm K, Dubrac A, et al. FGF-dependent metabolic control of vascular development. *Nature* 2017;**545**:224–8.
46. Diebold LP, Gil HJ, Gao P, Martinez CA, Weinberg SE, Chandel NS. Mitochondrial complex III is necessary for endothelial cell proliferation during angiogenesis. *Nat Metab* 2019;**1**:158–71.
47. Simmonds MA. A site for the potentiation of GABA-mediated responses by benzodiazepines. *Nature* 1980;**284**:558–60.
48. Bruning U, Morales-Rodriguez F, Kalucka J, et al. Impairment of angiogenesis by fatty acid synthase inhibition involves mTOR malonylation. *Cell Metab* 2018;**28**:866–80.
49. Willeit P, Skroblin P, Moschen AR, et al. Circulating microRNA-122 is associated with the risk of new-onset metabolic syndrome and type 2 diabetes. *Diabetes* 2017;**66**:347–57.
50. Wendel AA, Cooper DE, Ilkayeva OR, Muoio DM, Coleman RA. Glycerol-3-phosphate acyltransferase (GPAT)-1, but not GPAT4, incorporates newly synthesized fatty acids into triacylglycerol and diminishes fatty acid oxidation. *J Biol Chem* 2013;**288**:27299–306.